Absolute cross-section measurements for electron-impact ionization of Na-like ions—Mg^+, Al^{2+}, and Si^{3+}

D. H. Crandall and R. A. Phaneuf

Physics Division, Oak Ridge National Laboratory, Oak Ridge, Tennessee 37830

R. A. Falk, D. S. Belić,* and G. H. Dunn[†]

*Joint Institute for Laboratory Astrophysics, University of Colorado and National Bureau of Standards,
Boulder, Colorado 80309*

(Received 7 August 1981)

Measured cross sections for single ionization of Mg^+, Al^{2+}, and Si^{3+} by electron impact are reported. Crossed beams of electrons and ions have been employed to study the absolute cross sections as a function of collision energy in detail. Near threshold the cross sections for Mg^+ and Al^{2+} are roughly 70% of the predicted direct-ionization cross sections, while Si^{3+} is in reasonable agreement with the predictions. Contributions to the total cross section by indirect processes, principally inner-shell-excitation autoionization, are specifically identified in each case and compared with theoretical results. These comparisons demonstrate specific failures of the predictions which rely on addition of excitation cross sections to the direct-ionization cross section.

I. INTRODUCTION

Electron-impact ionization is obviously important in many physical phenomena, particularly any discharge or plasma. The basic ionization process has been long and actively studied, but a fully satisfying description of the problem remains elusive. Two aspects of the problem present particular difficulties: (1) proper description requires representation of three free particles in the final state; (2) in addition to direct ionization, other complex mechanisms can contribute to the ionization process. Representing these mechanisms requires detailed knowledge of atomic states (resonances) embedded in the continuum, their configuration mixing, coupling to the continuum, etc.

Studies of ionization along isoelectronic sequences provide some generalization of aspects associated with atomic structure. The Na-like ions are of particular interest because the single electron in the outer shell makes the problem somewhat simpler, while the relatively large number of electrons in the next lower shell provides an amplification to any contribution by inner-shell processes. Excitation of an inner-shell electron can populate levels of the ions which are higher in energy than the ionization potential. Decay of such resonances usually proceeds rapidly via autoionization so that the excitation event contributes to the ionization cross section. The term "excitation autoioniza-

tion" has been broadly adopted for this process, and a number of previous investigators[1−5] have recognized that Na-like ions are particularly good candidates for study of excitation autoionization.

In 1968, Bely[2] used a scaled Coulomb-Born theory to estimate the detailed effects of excitation autoionization for Na-like ions, finding an abrupt increase in the Mg^+ ionization cross section of nearly a factor of 2 at the threshold for the excitation $2p^6 3s \rightarrow 2p^5 3s\, 3p$. He predicted a monotonic increase of this effect along the isoelectronic sequence, so that Fe^{15+} was predicted to have a tenfold increase in the ionization cross section due to excitation autoionization. The fact that Bely significantly overestimated the autoionization contributions was soon revealed by the experiment of Martin, Peart, and Dolder[3] on Mg^+, which could not detect an excitation-autoionization increase in the ionization cross section in spite of sensitivity to an abrupt increase as small as 7%. In a more detailed Coulomb-Born calculation, Moores and Nussbaumer[4] subsequently predicted only a 20% increase in the ionization cross section due to autoionization resonances for Mg^+, but a significant discrepancy with the experiment remained.

Experimental evidence exists which demonstrates that excitation autoionization can dominate over direct ionization[6,7] and that the relative importance of this process increases along isoelectronic sequences.[8−10] However, the Na-like sequence re-

mains an interesting case for which the effect of autoionization should be significant and for which it is possible to study a number of members of the sequence experimentally. The present research is a study of the ionization of the first three ions of the Na-like sequence—Mg^+, Al^{2+}, Si^{3+}—in sufficient detail to provide insight into the discrepancy between experiment and theory. This paper presents experimental results. An accompanying paper[11] presents a theoretical analysis of the atomic structure together with distorted-wave calculations of the collisional excitation of individual autoionizing levels and branching ratios to the continuum for direct comparison with the experiment. From the details found experimentally and theoretically, specific strengths and weaknesses in our understanding of excitation autoionization can be identified.

II. EXPERIMENTAL TECHNIQUES

A. General

The experiments were performed with crossed beams of electrons and ions. The Mg^+ study used ions produced in a hot cathode, discharge-type ion source[12] and with crossed-beams apparatus described earlier.[10,13] The Al^{2+} and Si^{3+} measurements used ions from the ORNL-PIG (Ref. 14) ion source and crossed-beams apparatus also described earlier.[15] The electron gun in both experiments is as described by Taylor et al.[16,17]

Cross sections are determined from measured parameters through the standard[18] relationship for crossed beams:

$$\sigma = \frac{\mathscr{R}}{I_i I_e} \frac{qe^2 v_i v_e}{(v_i^2 + v_e^2)^{1/2}} \frac{\mathscr{F}}{D} , \tag{1}$$

where $\mathscr{R}$ is the count rate for ions of charge $q + 1$, I_i and I_e are the incident ion and electron currents, v_i and v_e are the ion and electron velocities, $\mathscr{F}$ is the form factor for the beams' overlap, D is the efficiency of detection of the ionized ions, q is the charge of the incident ion in units of e, and e is the electron unit of charge. Care must be taken to assure that the measured $\mathscr{R}$, I_i, I_e, and $\mathscr{F}$ reflect true quantities at the beams' interaction point.

B. Ion beams

The Mg^+ ions were produced by insertion of a solid piece of Mg into a standard discharge

source.[12] The heat from the ion source filament was sufficient to vaporize enough Mg to sustain the discharge in the source without additional gas feed. Ion currents of about 0.3 μA were obtained at the interaction region. The Al^{2+} ions were produced by inserting a rod of Al directly into the PIG source and operating the source discharge with CCl_4. The chlorine in contact with hot Al makes aluminum chloride which has a high enough vapor pressure to yield a significant amount in vapor phase. The technique is similar to that used previously to produce Be^+ ions[10,19] and will work for a number of metallic ions[7] in gas discharge. Al^{2+} currents of 0.1 to 0.3 μA were obtained at the collision center. The Si^{3+} ions were produced in the ORNL-PIG source by running the discharge on silane (SiH_4) gas. Ion currents of 0.1 μA were typical at the interaction region.

As already noted, the crossed-beams arrangement, charge-state analyzer, and particle detector for the Mg^+ measurements were all identical to those previously described,[10,13] and little further description will be given. For Al^{2+} and Si^{3+}, the apparatus and method are substantially as previously described,[15] but some changes deserve mention. The apparatus used for these measurements is shown schematically in Fig. 1. The main changes were the following: (1) another stage was added at the primary-beam output slit of the charge analyzer to further remove the primary-beam Faraday cup from the signal detector, and thus reduce background; (2) the exit slits for signal and primary beams were placed in positions for 2^+ charged primary beams and 3^+ product beams.
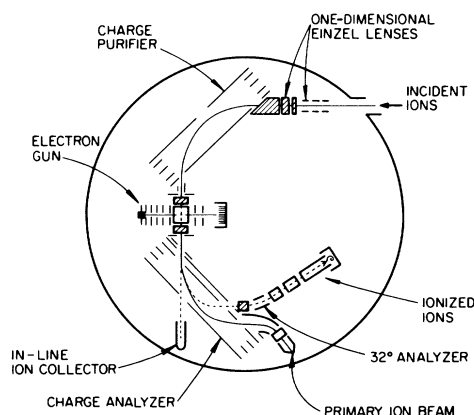

FIG. 1. Schematic of the crossed-beam collision chamber and ion beam analysis system viewed from above. Cross-hatched elements can provide vertical deflection of ions.

However, the primary-beam exit slit was made into an elongated hole such that when a 4^+ product beam was focused into the signal slit, a primary 3^+ beam would be collected in the Faraday cup.

The additional deflection of the primary beam together with a gold black[20] deposit on analyzer surfaces reduced background by an order of magnitude. However, background remains a problem and varies significantly with ion species. Table I shows background counts per nanoampere of primary current and signal-to-background ratio for several ions including those of this experiment (note again the Mg^+ measurements were obtained with separate apparatus). The Si^{3+} backgrounds are significantly worse than any other case. Tests indicate that cases of high background result from production of photons at surfaces impacted by the high-energy ions.

The elongated slit to allow measurement of both $2^+\rightarrow3^+$ and $3^+\rightarrow4^+$, with the same analyzer worked only marginally well. Transmissions were near 100% for the $2^+\rightarrow3^+$ case, but for Si^{3+} (the $3^+\rightarrow4^+$ case) it was found that only $80-90\%$ of the primary beam was measured. Careful measurements of the transmissions allowed correction of the data, and later checks with an analyzer constructed specifically for $3^+\rightarrow4^+$, where the transmission was near 100%, verified the accuracy of the corrected data. (Surprisingly, we found the new analyzer did not reduce noise levels for Si^{3+} significantly from those of Table I.)

Tests were made[15] to verify that quantities in Eq. (1) were measured correctly and that no extraneous effects gave misleading results. Careful inventories of ion beam currents along the path gave accurate transmissions within uncertainties to be discussed later. Tests for impurities in the ion beam (same q/m_i, but different m_i and q) were frequently performed as described in Ref. 15, and impurity levels were negligible during data collection. The test applied to detect space-charge modulation of backgrounds was measurement of the apparent cross section below ionization threshold.

C. Electron beam

The electron sources have been thoroughly described.[16,17] The interaction energies are determined from Eq. (8) in Ref. 17 with additional terms for Al^{2+} and Si^{3+}. For these two cases the ion velocity adds 0.4 eV to the collision energy for Al^{2+} at 20 keV and 0.8 eV for Si^{3+} at 45 keV where most data were taken. In addition, for these two ions the penetration of the vertical electrostatic deflection fields[15] shifts the average potential slightly. The electrostatic deflector plates are operated symmetrically with positive voltages on the top plates and negative voltages on the bottom plates. However, the electron and ion beams intersect slightly below the center line of these plates, so that a small negative potential shift is introduced. The applied voltages are somewhat higher for the faster Si^{3+} ions in this case. The estimated

TABLE I. Background counts per ion current and signal-to-background ratio (S/B) for several ions.

Ion	$\dfrac{B}{I_i}\left[\dfrac{s^{-1}}{nA}\right]^b$	Electron energy (eV)	S/B
Si^{3+}	111.0	95	0.01
		295	0.10
Ar^{3+}	9.6	95	0.50
		295	2.0
Al^{2+}	16.0	95	0.33
		245	0.69
C^{2+}	2.0	95	0.74
		245	2.30
$Mg^{+\ a}$	18.0	95	2.47
		245	5.68

[a]Mg^+ data involved separate apparatus.
[b]Currents are in *particle* nanoamperes.

shifts of electron energy in the collision region are roughly equal but opposite to the ion velocity components given above. Thus, the actual energies quoted here for Al^{2+} and Si^{3+} have not been corrected from the result given in Ref. 17 because the two additional terms approximately cancel. Based on previous calibrations and experience with the electron source and on the present agreement of experimental and theoretical ionization thresholds, the quoted electron energies are believed to be accurate (at good confidence) to within about ± 0.5 eV for Mg^+ data and to within about ± 0.7 eV for Al^{2+} and Si^{3+} data.

The spread in electron energy is important in the present data, since the excitation contributions are expected to appear as abrupt step increases in the ionization cross sections. For Mg^+ the energy spread in the resonance region should be about 0.5-eV full width at half maximum (FWHM) (Ref. 17) due to the combination of thermal energy spread at the cathode and space-charge effects. For the Al^{2+} and Si^{3+} case the penetration of the potentials from the vertical deflector plates results in a variation in space potential over the vertical extent of the beams. Previous measurements on excitation cross sections[21] indicated that the energy spread at 10 eV was about 3 eV, principally due to this field penetration. However, the height of the beams has been decreased by nearly a factor of 2, so that the variation in space potential should similarly decrease. It is estimated that the energy

spread in the resonance region is just below 2-eV FWHM for Al^{2+} and just above 2 eV for Si^{3+} and is dominated by the field penetration of the vertical deflectors.

D. Uncertainties

Cross sections are determined from averages of repeated measurements at a sequence of energies. A given energy may be repeated in separate cycles or on separate days (ion source retuned). During each data run, a specific benchmark energy was included in the sequence which was common to all runs (for Mg^+, Al^{2+}, and Si^{3+} the standard electron energies were 97.2, 242, and 292 eV, respectively). Careful absolute calibrations were made at the benchmark energies, and all data were renormalized using these points. These renormalization factors typically varied less than $\pm 2\%$. However, renormalization factors for the Si^{3+} data varied by as much as $\pm 12\%$ due to the problems with incomplete transmission of the primary ion beam. After the renormalization, measurements at a given energy are averaged to obtain the quoted cross section. For the present data, cross sections determined at energies differing by up to ± 0.5 eV for Mg^+ and Al^{2+} and by up to ± 3 eV for Si^{3+} were averaged together and are quoted at the average energy. Repeats of six or more trials are averaged in the present data. The standard deviation of the

TABLE II. Uncertainties.

Source	Mg$^+$	Uncertainty in % Al^{2+}	Si^{3+}
Statistical uncertainty (90% confidence level): typical value in % of peak cross section	± 1	± 3	± 5
Additional systematic uncertainty:			
Particle-counting efficiency	± 8	± 2	± 2
Transmission to signal ion counter	± 1	± 5	± 5
Background modulation	± 2	± 2	± 6
Incident ion current	± 1	± 2	± 6
Incident electron current	± 1	± 2	± 2
Form-factor evaluation	± 2	± 3	± 3
Uncertainty in velocities	± 0.5	± 1	± 1
Calibration vibrating reed electrometer	± 1		
Quadrature sum:			
Typical total % uncertainty (good confidence)	± 9	± 8	± 12

mean of these averages is generally in good agreement with counting statistics. Variations in the data due to fluctuation of form factor, detector efficiency, and transmission factors during data collection apparently become important at about the $\pm 1\%$ level. The standard deviation of the mean of the repeated trials is taken as representative of relative uncertainty in the present data.

Total absolute uncertainty described here as "good confidence" is taken as the quadrature sum of statistical and systematic uncertainties where both are at 90% confidence level or the equivalent. Systematic and typical total uncertainties are listed in Table II.

For the Mg^+ data the signal detector is a large area, electron multiplier which has less than 100% detection efficiency for the 1-keV ions. This detector is calibrated by measuring the absolute signal ion current with a vibrating reed electrometer using the multiplier as a Faraday cup, then comparing with counts in the multiplier mode. For Mg^+ it is this detector calibration which has the largest systematic uncertainty, while for Al^{2+} and Si^{3+} it is determination of transmission of ions through the analyzer which has greatest uncertainty.

The modulation of background due to focusing of the ion beam by the electron beam, which occurred in earlier work,[15] has been largely eliminated in the present data. A systematic uncertainty is included which is large enough to account for possible residuals of this effect as determined by measurements below threshold.

Measured cross sections and the relative uncertainties at one standard deviation of the mean are given in Table III.

III. RESULTS AND DISCUSSION

The measured cross sections presented in Table III are plotted in Figs. 2–7. A principal goal of the present study was determination of the role of excitation autoionization in total-ionization cross sections. Thus, a particular effort was made to measure the cross sections in detail near the energies where the autoionizing resonances were expected to occur.

A. Mg^+ case

Figure 2 shows the results for Mg^+ from threshold through the resonance region. The shape of the measured cross section is compared to the cal-

culation by Younger[22] of direct ionization in the distorted-wave approximation by plotting the theoretical values normalized to experiment at 30 eV, an energy before the onset of excitation autoionization. The resonance region is expanded in the figure for clarity. The calculations of excitation autoionization by Moores and Nussbaumer[4] and by Griffin et al.[11] clearly indicate abrupt rises in the ionization cross section. Since the energy spread of the incident electron beam in this Mg^+ case should be quite small (~ 0.5 eV) such abrupt rises should be apparent in the measurements. A small increase presumably due to excitation of the $2p^5 3s^2$ level does occur between 50 and 52 eV, but clearly the increase expected near 55 eV due to the $2p^5 3s 3p$ level is absent. In spite of the lack of definitive structure, a substantial average increase in the total-ionization cross section does occur in the resonance region, assuming the normalized distorted-wave calculation of Younger reflects the correct shape of the direct-ionization process in the resonance region. At 70 eV, before onset of direct inner-shell ionization, the measured cross section is 18% greater than the estimate of the direct ionization—an overall increase approximately equal to the predicted total excitation-autoionization contribution. The discrepancies between theory and experiment are discussed in more detail by Griffin et al.,[11] but the result obtained by simply adding excitation autoionization to the direct ionization is not in satisfactory agreement with the experiment. The present results are more precise and provide more detail, but are in agreement with the earlier results of Martin, Peart, and Dolder.[3]

Figure 3 shows comparison of the absolute values of predicted and measured cross sections for Mg^+ over a broad energy range. The Lotz estimate is obtained using only the single Lotz[23] parameter $a = 4.5 \times 10^{-14}$ cm^2. Lotz gives a formula with different fitting parameters for each subshell[23,24]; but for the present cases, the results differ only slightly from the simpler and more widely used single-parameter formula. Our results are compared with measurements of Martin et al.[3] The two experiments are seen to be in reasonable absolute agreement and only a little lower than the distorted-wave and Coulomb-Born calculations.

B. Al^{2+} case

For the Al^{2+} case shown in Figs. 4 and 5, the anticipated excitation-autoionization structures are more apparent in the data and do occur as sharp

TABLE III. Measured cross sections for single ionization of Mg^+, Al^{2+}, and Si^{3+} by electron impact. Values in parentheses are one standard deviation on counting statistics and are taken as representative of relative uncertainties.

Mg$^+$		Al^{2+}		Si^{3+}	
E (eV)	σ (10^{-18} cm^2)	E (eV)	σ (10^{-18} cm^2)	E (eV)	σ (10^{-18} cm^2)
15.2	6.10(0.33)	28.9	1.15(0.59)	54	+ 1.01(0.70)
17.3	19.08(0.30)	31.0	2.56(0.42)	71	3.76(0.60)
19.3	26.98(0.61)	33.0	2.84(0.43)	81	4.83(0.56)
21.3	32.45(0.08)	35.0	3.72(0.42)	87	5.37(0.43)
23.3	36.10(0.47)	36.6	5.48(0.35)	95	5.34(0.33)
25.2	38.83(0.28)	38.6	5.38(0.46)	102	7.29(0.29)
27.2	39.88(0.24)	40.6	6.93(0.26)	107	6.96(0.29)
29.2	41.31(0.20)	42.6	6.78(0.29)	111	5.57(0.28)
31.3	42.03(0.46)	44.5	7.94(0.35)	115	6.55(0.28)
33.2	42.17(0.32)	46.3	7.93(0.21)	121	7.00(0.27)
35.3	42.32(0.31)	48.5	7.93(0.32)	127	6.91(0.26)
37.7	41.02(0.15)	50.7	8.44(0.23)	133	7.64(0.37)
39.7	41.56(0.11)	52.4	8.68(0.29)	139	8.73(0.42)
41.7	40.48(0.11)	54.4	8.45(0.29)	144	8.74(0.27)
43.8	40.42(0.14)	56.4	8.85(0.22)	150	8.31(0.42)
45.8	39.97(0.12)	58.3	9.05(0.27)	158	9.54(0.32)
47.8	39.84(0.13)	60.3	8.96(0.26)	173	9.19(0.50)
49.8	40.03(0.16)	61.6	9.07(0.23)	192	10.19(0.36)
51.8	40.43(0.14)	64.3	8.84(0.28)	213	9.97(0.40)
53.8	40.11(0.17)	66.1	8.93(0.15)	242	10.67(0.40)
55.8	39.96(0.16)	68.1	9.22(0.20)	292	10.98(0.18)
57.8	39.90(0.10)	70.7	9.09(0.16)	341	10.45(0.99)
59.8	39.58(0.08)	72.0	8.96(0.20)	391	10.73(0.35)
61.8	39.50(0.07)	74.0	9.51(0.15)	488	11.03(0.19)
63.8	39.35(0.08)	75.9	9.78(0.15)	636	8.55(0.21)
		77.9	10.28(0.19)	786	8.80(0.24)
65.8	39.18(0.06)	80.3	10.00(0.25)	989	7.28(0.14)
67.8	39.11(0.10)	82.1	10.16(0.25)	1492	6.37(0.35)
69.8	39.34(0.24)	83.5	9.80(0.23)		
71.8	39.32(0.23)	85.5	10.87(0.23)		
73.8	39.08(0.23)	87.9	11.19(0.31)		
75.8	39.11(0.26)	90.1	10.78(0.25)		
77.8	38.77(0.17)	91.6	10.61(0.37)		
87.2	38.28(0.28)	95.4	11.32(0.14)		
97.2	38.31[a]	97.6	11.02(0.22)		
117	37.67(0.36)	99.6	10.99(0.21)		
138	37.73(0.34)	101	11.06(0.21)		
158	38.09(0.33)	103	11.72(0.20)		
179	38.20(0.33)	105	11.43(0.17)		
200	37.84(0.27)	107	11.41(0.20)		
220	36.70(0.26)	109	11.44(0.18)		
241	35.50(0.26)	111	11.93(0.17)		
262	34.04(0.25)	114	11.88(0.14)		
282	32.69(0.25)	118	12.47(0.20)		
303	31.36(0.26)	121	12.70(0.20)		
323	30.22(0.26)	125	12.37(0.11)		
344	29.26(0.24)	130	12.65(0.18)		
364	28.40(0.31)	135	12.58(0.14)		

TABLE III. (Continued.)

	Mg$^+$		Al^{2+}		Si^{3+}	
E (eV)	σ (10^{-18} cm^2)	E (eV)	σ (10^{-18} cm^2)	E (eV)	σ (10^{-18} cm^2)	
385	27.78(0.20)	145	12.68(0.17)			
406	27.25(0.19)	154	12.82(0.21)			
		175	13.93(0.13)			
		194	13.66(0.17)			
		242	14.07(0.08)			
		341	13.41(0.15)			
		492	12.42(0.17)			
		744	11.29(0.15)			
		994	9.23(0.26)			

^{a}Absolute — at 97.2 38.31(1.76).

steps within the estimated 2-eV experimental energy spread. In Fig. 4 the normalized distorted-wave calculations of direct ionization by Younger[22] (or normalized scaled Coulomb-Born results of Golden et al.[25]) again fit the near-threshold results well and serve as a guide for the expected direct ionization in the resonance region. The data are suffi-

ciently detailed to provide accurate comparison with excitation theory for the excitation-autoionization contribution, and detailed comparison is presented in the accompanying paper.[11] However, the comparison is qualitatively similar to
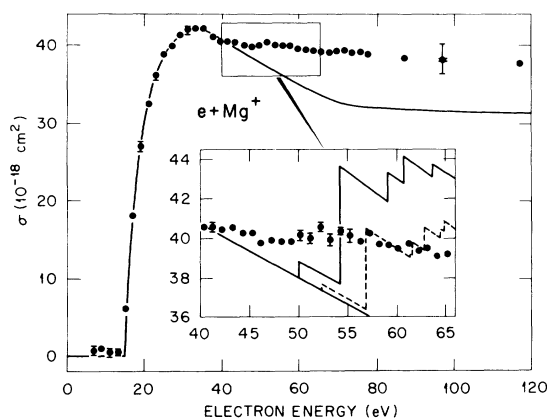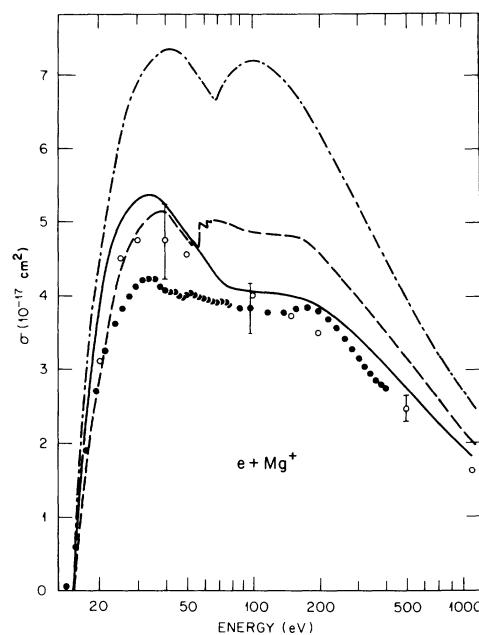

FIG. 2. Electron-impact ionization of Mg$^+$ near threshold. Data points are present experimental values with relative uncertainties shown at one standard deviation and with bars smaller than the points where not shown. The outer bar at 97.2 eV points is absolute uncertainty at good confidence (90% confidence-level equivalent). The solid line is distorted-wave theory for direct ionization by Younger (Ref. 22) normalized to the experiment at 30 eV by multiplying Younger's results by 0.78. The inset shows the resonance region in detail with the experimental results at 1-eV intervals as originally obtained and shows the excitation-autoionization results of Moores and Nussbaumer (Ref. 4) (dashed line) and of Griffin et al. (Ref. 11) (solid line) added to the normalized distorted-wave result.

FIG. 3. Electron-impact ionization of Mg$^+$ over a broad energy range. Solid points are present experiment with relative uncertainties smaller than the points and typical good-confidence total uncertainty shown at 97.2 eV. Open points are experiments of Martin et al. (Ref. 3); solid curve is direct-ionization calculation by Younger (Ref. 22); dashed curve is Coulomb-Born calculation of Moores and Nussbaumer (Ref. 4) including excitation autoionization; and dot-dashed curve is the Lotz prediction (Ref. 23).
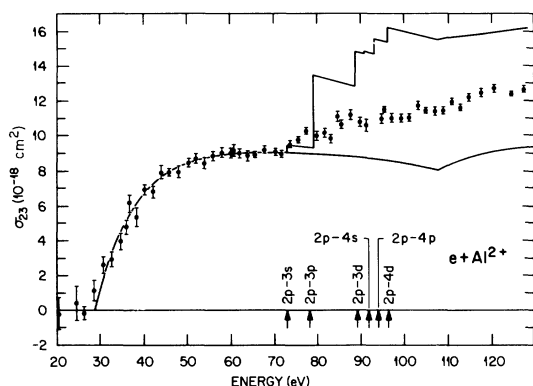
FIG. 4. Electron-impact ionization of Al^{2+} near threshold. The solid curve is distorted-wave calculation of direct ionization by Younger (Ref. 22), normalized to the experiment at 70 eV by multiplying Younger's results by 0.65. The distorted-wave excitation of Griffin *et al.* (Ref. 11) is added to the Younger direct-ionization results with arrows indicating center-of-gravity energies for excitation of a $2p$ electron to final orbital nl.
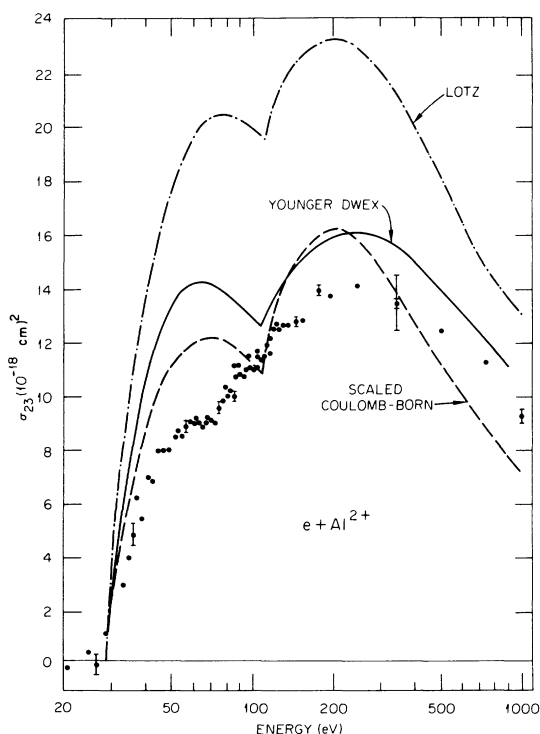

FIG. 5. Electron-impact ionization of Al^{2+} over a broad energy range. Points are present experimental results with typical relative uncertainty at one standard deviation except at 242 eV where outer bar is good-confidence absolute uncertainty. Solid curve is distorted-wave theory (Ref. 22); dashed curve is scaled Coulomb-Born theory (Ref. 25); and dot-dashed curve is Lotz-formula prediction (Ref. 23).

that for Mg^+ in that the largest predicted excitation-autoionization step $(2p^5 3s\,3p)$ is effectively absent, and the overall increase in the ionization cross section is smaller than predicted by excitation theory. The increase in measured ionization cross section over the normalized distorted-wave calculation is about 40% at 104 eV.

The absolute comparison of experiment and theory (direct process only) over a broad energy range is shown for Al^{2+} in Fig. 5. The single-parameter Lotz formula again severely overestimates the cross section. Near 60 to 70 eV, just before the onset of excitation autoionization, the distorted-wave and scaled Coulomb-Born calculations are also in poor agreement with the experimental results, but at higher energy the excitation contribution fortuitously results in better agreement with these theories which—it is emphasized again—do not include excitation autoionization.

C. Si^{3+} case

For the Si^{3+} case shown in Figs. 6 and 7, the experimental data are clearly of lesser precision. The fairly good agreement of experiment and distorted-wave theory near threshold in Fig. 6 did not require any normalization of the theory in this case. The excitation-autoionization resonances are apparent in the data at the predicted[11] energies. The total excitation contribution, estimated from the difference between measured ionization cross section and the distorted-wave direct-ionization prediction, is 65% at 145 eV.

Figure 7 shows comparison of experiment and theory (direct process only) over the broad energy range. Interestingly, the excitation contribution steps the experimental data from good agreement with the distorted-wave and Coulomb-Born direct-ionization calculations up to good agreement with the Lotz formula. Of course, this high-energy agreement with the Lotz formula is accidental and should not prevail generally for more highly ionized species in the sequence.

D. General trends

Some indication of improving agreement for direct ionization between theory and experiment as charge state increases has been noted previously,[8,9] though other work[10,25] makes this conclusion less firm. In the present case, DW theory is 27%

higher for Mg^+, 48% higher for Al^{2+}, and is in agreement with experiment for Si^{3+} in the region just before excitation autoionization sets in. Thus, there is a suggestion of improving agreement with higher charge state, but again the trend is erratic and no firm conclusion can be drawn.

The role of excitation autoionization and its relative change in importance with increasing ionic charge along an isoelectronic sequence are also not so well established. Experimental[8–10] and theoretical[26,27] excitation contributions diverge somewhat for the Li-like sequence. For the present Na-like ions a comparison of theory and experiment for the excitation-autoionization contribution is given in Table IV. The experimental excitation part is obtained from Figs. 2, 4, and 6 by subtracting the normalized distorted-wave theory from the total measured ionization cross section. The percentage increase given in the tables is the excitation contribution divided by the normalized distorted-wave theory to represent the direct-ionization com-
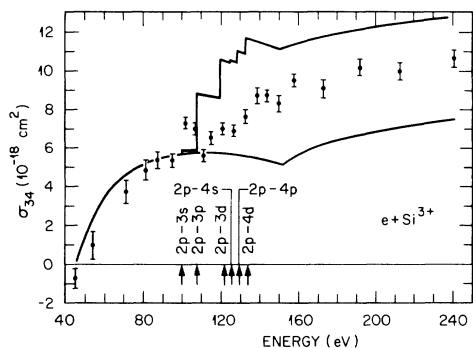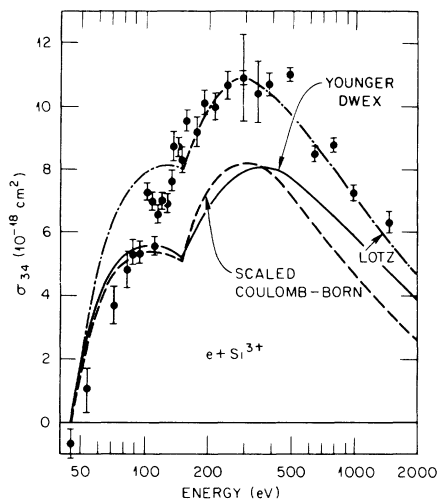

FIG. 7. Electron-impact ionization of Si^{3+} over a broad energy range. Points are present experimental data with relative uncertainty at one standard deviation; except at 292 eV the outer error bar is good-confidence absolute uncertainty. Solid curve is distorted-wave theory by Younger (Ref. 22); dashed curve is scaled Coulomb-Born theory (Ref. 25); and dot-dashed curve is Lotz-formula prediction (Ref. 23).

ponent. The trend of increasing relative importance of excitation autoionization along this sequence is qualitatively as predicted by theory, but should be followed to higher ion stages by detailed comparisons of theory and experiment. However, the present comparisons suggest either that excitation theory is inadequate or that the contribution of indirect processes to total ionization is not adequately described by simple addition of excitation and ionization cross sections. Simple power-law extrapolation of the experimental data in Table IV would indicate that by Fe^{15+}, the excitation autoionization is about four times the direct cross section. Such distant extrapolation is, of course, very uncertain.

Figure 8 shows the rate coefficients obtained in each case for Maxwellian electron energy distribution.[28] As in Figs. 3, 5, and 7 the theoretical
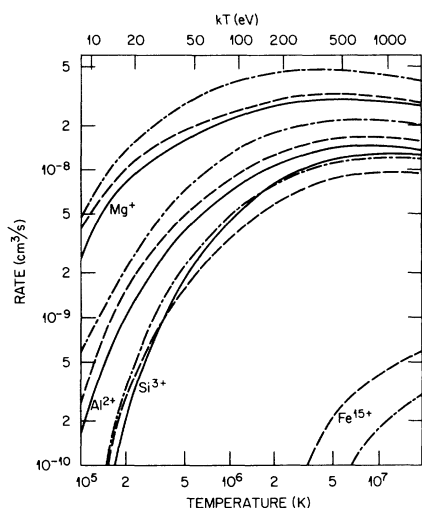

FIG. 6. Electron-impact ionization of Si^{3+} near threshold. Points are present experiment with relative uncertainty at one standard deviation. Solid curve is distorted-wave theory for direct ionization by Younger (Ref. 22) without any normalization in this case. The curve added to the distorted-wave result is the excitation autoionization by Griffin et al. (Ref. 11).

TABLE IV. The excitation-autoionization component of the ionization cross sections at energies just below onset of direct inner-shell ionization. Theoretical results are from the accompanying paper of Griffin et al. (Ref. 11).

Ion	Energy (eV)	Experimental excitation		Theoretical excitation	
		$\sigma(10^{-18}$ cm$^2)$	% inc.	$\sigma(10^{-18}$ cm$^2)$	% inc.
Mg^+	70	6.0	18	8.9	26
Al^{2+}	104	3.3	40	7.1	88
Si^{3+}	145	3.5	65	5.8	109

FIG. 8. Rate coefficients for ionization of Mg^+, Al^{2+}, Si^{3+}, and Fe^{15+}. Solid curves are derived from present experimental results. Theoretical results, including direct ionization only: dashed curves from the distorted-wave ionization results of Younger (Ref. 22) and dot-dashed curves are Lotz result (Ref. 23). The short-dashed curve for Fe^{15+} is obtained from the cross-section prediction of LaGattuta and Hahn (Ref. 29).

values plotted for Mg^+, Al^{2+}, and Si^{3+} in Fig. 8 are for the direct process only. The trends established by the cross-section comparisons of Figs. 2−7 are somewhat smoothed out in the rate coefficient, but it remains apparent that indirect contributions have the greatest relative effect on the Si^{3+} rate coefficient. For comparison and to emphasize the nature of the continuing trend, the rate coefficient for Fe^{15+} from the Lotz formula and from recent calculations of LaGattuta and Hahn[29] are

also shown. These recent calculations for Fe^{15+} include not only excitation autoionization but also contributions for dielectronic recombination—double autoionization. Just below each of the excited states relevant in excitation autoionization there is a series of dielectronic recombination levels, many of which can decay by Auger emission of two free electrons. When this occurs the ionization cross section is enhanced by dielectronic recombination—double autoionization as well as by excitation autoionization. Thus Fig. 8 illustrates that indirect processes are expected to significantly enhance ionization rates for members of the Na-like isoelectronic sequence between Si^{3+} (for which the rate deduced from the experimental cross section shows such enhancement) and Fe^{15+}, where the predicted enhancement is greater than a factor of 2.

ACKNOWLEDGMENTS

*Permanent address: Department of Physics, Faculty of Natural and Mathematical Science, Belgrade, P.O. Box 57.
†Staff member, Quantum Physics Division, National Bureau of Standards.

[1]L. Goldberg, A. K. Dupree, and J. W. Allen, Annu. Rev. Astron. Astrophys. 28, 589 (1965).
[2]O. Bely, J. Phys. B 1, 23 (1968).
[3]S. O. Martin, B. Peart, and K. Dolder, J. Phys. B 1, 537 (1968).
[4]D. L. Moores and H. Nussbaumer, J. Phys. B 3, 161 (1970).
[5]R. D. Cowan and J. B. Mann, Astrophys. J. 232, 940 (1979).
[6]B. Peart and K. T. Dolder, J. Phys. B 1, 872 (1968).
[7]R. A. Falk, G. H. Dunn, D. C. Griffin, C. Bottcher, M. S. Pindzola, D. C. Gregory, and D. H. Crandall, Phys. Rev. Lett. 47, 494 (1981).
[8]D. H. Crandall, R. A. Phaneuf, B. E. Hasselquist, and D. C. Gregory, J. Phys. B. 12, L249 (1979).
[9]D. H. Crandall, Phys. Scr. 23, 153 (1981).
[10]R. A. Falk and G. H. Dunn (unpublished).
[11]D. C. Griffin, C. Bottcher, and M. S. Pindzola, Phys. Rev. A 25, 154 (1982), paper II.
[12]M. Menzinger and L. Wahlin, Rev. Sci. Instrum. 40, 102 (1969).
[13]W. T. Rogers, G. Stefani, R. Camilloni, G. H. Dunn, A. Z. Msezane, and R.J.W. Henry, Phys. Rev. A (in

press).

[14]M. L. Mallory and D. H. Crandall, IEEE Trans. Nucl. Sci. <u>NS-23</u>, No. 2, 1069 (1976).

[15]D. H. Crandall, R. A. Phaneuf, and P. O. Taylor, Phys. Rev. A <u>18</u>, 1911 (1978).

[16]P. O. Taylor, K. T. Dolder, W. E. Kauppila, and G. H. Dunn, Rev. Sci. Instrum. <u>45</u>, 538 (1974).

[17]P. O. Taylor and G. H. Dunn, Phys. Rev. A <u>8</u>, 2304 (1973).

[18]Some reviews: M.F.A. Harrison, J. Appl. Phys. <u>17</u>, 371 (1966); G. H. Dunn, in *Atomic Physics,* edited by V. W. Hughes, V. W. Cohen, and F.M.S. Pichanick (Plenum, New York, 1969), p. 417; K. T. Dolder and B. Peart, Rep. Prog. Phys. <u>39</u>, 693 (1976).

[19]P. O. Taylor, R. A. Phaneuf, and G. H. Dunn, Phys. Rev. A <u>22</u>, 435 (1980).

[20]L. Harris and J. K. Beasley, J. Opt. Soc. Am. <u>42</u>, 134 (1952).

[21]D. C. Gregory, G. H. Dunn, R. A. Phaneuf, and D. H. Crandall, Phys. Rev. A <u>20</u>, 410 (1979).

[22]S. M. Younger (unpublished).

[23]W. Lotz, Z. Phys. <u>220</u>, 466 (1969).

[24]W. Lotz, Z. Phys. <u>216</u>, 241 (1968).

[25]L. B. Golden and D. H. Sampson, J. Phys. B <u>10</u>, 2229 (1977); see also D. L. Moores, L. B. Golden, and D. H. Sampson, *ibid.* <u>13</u>, 385 (1980).

[26]D. H. Sampson and L. B. Golden, J. Phys. B <u>12</u>, L785 (1979).

[27]R.J.W. Henry, J. Phys. B <u>12</u>, L309 (1979).

[28]D. H. Crandall, G. H. Dunn, A. Gallagher, D. G. Hummer, C. V. Kunasz, D. Leep, and P. O. Taylor, Astrophys. J. <u>191</u>, 789 (1974).

[29]K. J. LaGattuta and Y. Hahn, Phys. Rev. A <u>24</u>, 2273 (1981).